Advances in Water Resources 129 (2019) 118–130

Contents lists available at ScienceDirect

Advances in Water Resources

journal homepage: www.elsevier.com/locate/advwatres

A general Beerkan Estimation of Soil Transfer parameters method predicting hydraulic parameters of any unimodal water retention and hydraulic conductivity curves: Application to the Kosugi soil hydraulic model without using particle size distribution data

J. Fernández-Gálvez[a,b,1,*], J.A.P. Pollacco[b], L. Lassabatere[c], R. Angulo-Jaramillo[c], S. Carrick[b]

[a] Department of Regional Geographic Analysis and Physical Geography, University of Granada, C/ Profesor Clavera, Granada 18071, Spain
[b] Manaaki Whenua – Landcare Research, Lincoln 7640, New Zealand
[c] Univ Lyon, Université Claude Bernard Lyon 1, CNRS, ENTPE, UMR5023 LEHNA, Vaulx en Velin, Lyon 69518, France

ARTICLE INFO

Keywords:
Soil hydraulic properties
Single ring infiltration experiments
BEST (Beerkan Estimation of Soil Transfer parameters)
Kosugi hydraulic parameters
van Genuchten hydraulic parameters
Quasi-exact implicit formulation

ABSTRACT

Soil hydraulic characterization is crucial to describe the retention and transport of water in soil, but current methodologies limit its spatial applicability. This paper presents a cost-effective general Beerkan Estimation of Soil Transfer parameters (BEST) methodology using single ring infiltration experiments to derive soil hydraulic parameters for any unimodal water retention and hydraulic conductivity functions. The proposed method relies on the BEST approach. The novelty lies in the use of Kosugi hydraulic parameters without need for textural information. In addition, the method uses a quasi-exact formulation that is valid for all times, which avoids the use of approximate expansions and related inaccuracy. The new BEST methods were tested against numerically generated data for several contrasting synthetic soils, and the results show that these methods provide consistent hydraulic functions close to the target functions. The new BEST method is accurate and can use any water retention and hydraulic conductivity functions.

1. Introduction

Water resource management depends on the predictive ability of spatially distributed hydrological models, which require dense information on the sub-grid spatial variability of soil hydraulic parameters describing the Water Retention, $\theta(h)$, and the Hydraulic Conductivity, $K(\theta)$, Functions, referred to as WRHCFs. The direct determination of $\theta(h)$ and $K(\theta)$ is based on sampling and laboratory methods that are precise and reliable, but scale limited. Laboratory approaches are often expensive, tedious, time-consuming, require specialist equipment and therefore are rather unrealistic for the large-scale characterization of soil hydraulic properties, particularly limiting for developing countries and non-research organisations. To circumvent these limitations, soil pedotransfer functions have been widely used to estimate soil hydraulic properties (van Looy et al., 2017) by using readily available measurements of soil particle size distribution (PSD) (e.g. Nasta et al., 2013a,b), soil bulk density, and organic carbon (e.g. Balland and Pollacco, 2008; Pollacco, 2008). Other explanatory variables include soil order classification, texture, and basic information from functional horizon descriptions (McNeill et al., 2018). However, the accuracy of deriving the hydraulic parameters from pedotransfer functions is constrained by local calibration, and they are less accurate than laboratory methods (e.g. Patil and Singh, 2016).

Another approach involves utilizing water infiltration techniques to characterize soil hydraulic parameters (Angulo-Jaramillo et al., 2016). Several approaches and methods have been developed based on a large array of water infiltration devices. Among these, the Beerkan Estimation of Soil Transfer parameters, referred to as the BEST method, was developed to derive the entire set of hydraulic parameters from Beerkan experiments (Angulo-Jaramillo et al., 2016; Lassabatere et al., 2006). The BEST approach involves directly measuring the initial soil water content (θ_{ini} [L^3L^{-3}]), the soil bulk density used to derive the saturated soil water content (θ_S [L^3L^{-3}]), the PSD, and the cumulative infiltration through a single ring under near-zero pressure head (I [L]).

Three main BEST methods were developed, including the original one (Lassabatere et al., 2006), its adaptation to coarse soils (Yilmaz et al., 2013), and its adaptation to those cases when only the final steady water infiltration can be obtained (Bagarello et al., 2014). All these methods consider the van Genuchten (1980) water

* Corresponding author.
E-mail address: jesusfg@ugr.es (J. Fernández-Gálvez).
[1] Permanent address: Department of Regional Geographic Analysis and Physical Geography, University of Granada, C/ Profesor Clavera, Granada 18071, Spain.

https://doi.org/10.1016/j.advwatres.2019.05.005
Received 22 October 2018; Received in revised form 22 April 2019; Accepted 15 May 2019
Available online 16 May 2019

Table 1
Descriptions of $S_e(h)$, $K(S_e)$, and $d\theta/dh$ equations for Kosugi and van Genuchten models, respectively.

Soil water retention, $S_e(h)$ =			
Kosugi (1996)	$\frac{1}{2} ERFC\left[\frac{\ln h - \ln h_{kg}}{\sigma\sqrt{2}}\right]$	erfc is the complementary error function, where ln h_{kg} [L] and σ [–] represent the mean and standard deviation of ln h, respectively.	[t1]
van Genuchten (1980)	$\begin{cases}\left[1+\left(\frac{h}{h_{vg}}\right)^n\right]^{-m} \\ m = 1 - k_m/n\end{cases}$	h_{vg} [L] is associated with the inflection point of the water retention curve; n [–] (>1) and m [–] (<1) are shape parameters related to the pore-size distribution; $k_m = 1$ [–] follows the assumption of Mualem and $k_m = 2$ [–] follows the assumption of Burdine.	[t2]
Unsaturated hydraulic conductivity, $K(S_e)$ =			
Kosugi (1996)	$K_s \sqrt{S_e}\left\{\frac{1}{2} ERFC\left[ERFC^{-1}\left(2(S_e)+\frac{\sigma}{\sqrt{2}}\right)\right]^2\right.$	FALSE	[t3]
van Genuchten (1980)	$K_s \sqrt{S_e}\left[1-\left(1-S_e^{\frac{1}{m}}\right)^m\right]^{\frac{2}{k_m}}$	This equation results from the application of the Mualem capillary model to the van Genuchten model.	[t4]
Brooks and Corey (1964)	$K_s S_e^{\eta}$	In BEST methods, the exponent is related to the shape parameter n $\eta = \frac{2}{m\,n} + 2 + p$, where p is a tortuosity parameter equally to 1 (Burdine condition)	[t5]
$\frac{d\theta}{dh}$ =			
Kosugi (1996)	$\frac{\theta_s - \theta_r}{\sqrt{2\,\pi}\,\sigma\,h} \mathrm{EXP}\left[-\frac{(\ln h - \ln h_{kg})^2}{2\,\sigma^2}\right]$		[t6]
van Genuchten (1980)	$\frac{m(\theta_s-\theta_r)}{h_{vg}(1-m)}\left(\frac{h}{h_{vg}}\right)^{nm}\left(1+\left(\frac{h}{h_{vg}}\right)^n\right)^{-m-1}$		[t7]

retention curve $\theta(h)$ with the Burdine condition (k_m = 2) and the Brooks and Corey (1964) hydraulic conductivity function $K(\theta)$ (Table 1). The residual water content, θ_r [L^3L^{-3}], is set at zero. The saturated water content, θ_S, is equal to the soil porosity. The shape parameter, n [–], related to the van Genuchten model (Table 1), referred to as VG, is estimated from the PSD using the pedotransfer functions detailed in Lassabatere et al. (2006). Lastly, the remaining scale parameters for hydraulic pressure head, h_{vg} [L], and the saturated hydraulic conductivity, K_S [L T^{-1}], are derived from analysis of the infiltration data, with the analytical approximate expansions proposed by Haverkamp et al. (1994) for steady and transient states.

The differences between the three models described above involve how they fit the transient and steady-state models to the experimental infiltration curves. The main advantage of the BEST approach is that the overall experiments are relatively fast, robust, low-cost, and easy to perform. In addition, field infiltration techniques sample large volumes of undisturbed soils, thus improving the representativeness and accuracy of the estimated effective parameters in comparison to laboratory methods using small cores (e.g. Anderson and Bouma, 1973; Carrick et al., 2010; Lauren et al., 1988).

The BEST method has been applied worldwide (e.g. Angulo-Jaramillo et al., 2016; Bagarello et al., 2014, 2017; Di Prima, 2015, 2016; Lassabatere et al., 2006, 2013) but presents the following drawbacks:

- It only works with a specific set of hydraulic functions (the van Genuchten (1980) model with Burdine condition for $\theta(h)$, and the Brooks and Corey (1964) model for $K(\theta)$) that are not frequently used for modelling or even implemented in major modelling tools and software. For instance, this set of WRHCFs is not implemented in HYDRUS, which is one of the most frequently used numerical models for flow and solute transfer (Šimůnek et al., 2016). Consequently, the WRHCFs estimated by the current BEST methods are not easy to use.
- It requires knowing the soil PSD in order to infer the shape parameter, n. This becomes limiting for widespread application, as accurate PSD analysis requires specialist equipment and skills. In addition, the assumptions behind the pedotransfer functions proposed by Lassabatere et al. (2006) are not valid for all soils and are potentially questionable.
- The BEST methods make use of approximate expansions that are valid only over restricted ranges and when used outside of their time validity intervals may lead to erroneous estimations.

To overcome these drawbacks described above, we propose a generalization of the existing versions of BEST (Lassabatere et al., 2009) to enable prediction of hydraulic parameters of any WRHCFs. Moreover, the use of the Kosugi hydraulic functions allows for the estimate of hydraulic parameters without PSD data. The robustness of the proposed universal BEST method is assessed by comparing the predictions of sorptivity (S [L $T^{-0.5}$]), K_S and $\theta(h)$ derived by (a) the van Genuchten (1980) model with the Mualem condition (k_m = 1) for the $\theta(h)$ and $K(\theta)$ (referred as VG WRHCFs described in Table 1); and (b) the Kosugi (1996) $\theta(h)$ and $K(\theta)$ models (referred as KG WRHCFs described in Table 1) with the robust and accurate quasi-exact implicit (QEI) formulation proposed by Haverkamp et al. (1994). We chose to compare to the QEI formulations (e.g. Lassabatere et al., 2009; Latorre et al., 2015; Moret-Fernández and Latorre, 2017; Parlange et al., 1982) rather than to the original BEST formulation (Lassabatere et al., 2009), which was derived from the QEI formulation, since the BEST formulation is always less accurate and requires PSD measurements.

The manuscript is organised as follows: Section 2 outlines the theory behind the proposed new BEST methods; Section 3 presents the methods for the numerical computations; Section 4 assesses the validity of the new BEST methods; Section 5 summarises the key conclusions and Section 6 summarizes recommendations for future work to improve the soil hydraulic parameterization estimated from BEST methods.

2. Theory

Previous BEST methods have relied on the van Genuchten (1980) model with Burdine condition, along with the Brooks and Corey (1964) model (Table 1), estimating the full set of hydraulic parameters (θ_r, θ_S, h_{vg}, K_S, n, η) based on the following: (1) θ_r is considered to be zero and θ_S is equal to the soil porosity estimated from bulk density measurements; (2) the shape parameter, n, is estimated from soil PSD and used to derive the shape parameter η; (3) the scale parameter, K_S, is optimized concomitant with soil sorptivity, S, by fitting the experimental cumulative infiltration to the analytical models; and (4) the scale parameter, h_{vg}, is estimated from previous estimates of S and K_S.

In the new versions we use the Kosugi functions (KG WRHCFs) (Table 1), with the associated set of hydraulic parameters (θ_r, θ_S, h_{kg}, K_S, σ), but the proposed approach can work with any hydraulic model. As in previous BEST methods, θ_r is considered to be zero and θ_S is equal to the soil porosity, estimated from bulk density measurements. The model used to fit the data is directly described as a function of the soil hydraulic

parameters, including the sorptivity parameter, S. Consequently, the fit allows the direct estimation of parameters (h_{kg}, K_S, σ). When PSD data are not available, a particular approach is proposed for the Kosugi model using a relation between h_{kg} and σ that is used to define an objective function (OF) with only two input variables, reducing non-uniqueness of the inverted hydraulic parameters.

In the following, first we present the model and the objective functions that are used to fit experimental cumulative infiltrations in order to derive the hydraulic parameters in the new BEST methods. Then we describe how to derive the remaining hydraulic parameters from S and K_S.

2.1. Using the quasi-exact implicit formulation in the BEST method, $BEST_{QEI}$

The $BEST_{QEI}$ method uses the model developed by Haverkamp et al. (1990, 1994) for the 1D cumulative infiltration, I_{1D}[L], under a constant zero or negative hydraulic pressure head at the surface into a soil with uniform initial water content. The model was extended by Smettem et al. (1994) to the case of 3D cumulative infiltration, I_{3D}, through a disc source, leading to the following expression:

$$I_{3D}(t) = I_{1D}(t) + \frac{\gamma}{\check{r}\Delta\theta} S^2 t \tag{1a}$$

$$\frac{2\Delta K^2}{S^2} t = \frac{1}{(1-\beta)}\left[\frac{2\Delta K}{S^2}\left(I_{1D}(t) - K_0 t\right) - \ln\left(\frac{\exp\left(2\beta\frac{\Delta K}{S^2}\left(I_{1D}(t) - K_0 t\right)\right) + \beta - 1}{\beta}\right)\right] \tag{1b}$$

where the subscripts 1D and 3D refer to the one-dimensional and three-dimensional cumulative infiltrations, respectively; $\Delta\theta = \theta_S - \theta_0$ [$L^3\ L^{-3}$] corresponds to the difference between the final saturated water content, and the initial water content; $\check{r}$ [L] is the ring radius of the infiltrometer; and γ is a geometric shape parameter fixed at 0.75 (Haverkamp et al., 1994). The term $\frac{\gamma}{\check{r}\Delta\theta}$ if often denoted as A [L^{-1}] (Lassabatere et al., 2013). In Eq. (1b), $\Delta K = K_S - K_0$ [$L\ T^{-1}$], which is the difference between final saturated hydraulic conductivity and the initial hydraulic conductivity, $K_0 = K(\theta_0)$; and β is an integral shape parameter, typically fixed at 0.6 (Haverkamp et al., 1994; Parlange et al., 1982).

The set of Eq. (1a) and (b) yields the 3D cumulative infiltration into a single ring infiltrometer and is referred to as the QEI model. This model is valid for all times and can be written in a scaled from, as proposed by Lassabatere et al. (2009) and Varado et al. (2006):

$$I_{3D}(t) = \frac{S^2}{2\Delta K} I^*\left(\frac{S^2}{2(\Delta K)^2} t\right) + \left(K_0 + \frac{\gamma}{\check{r}\Delta\theta} S^2\right) t \tag{2a}$$

with $I^*(t^*)$ being implicitly defined as the root of the following equation for any given t^*:

$$t^* = \frac{1}{(1-\beta)}\left(I^*(t^*) - \ln\left(\frac{\exp(\beta\, I^*(t^*)) + \beta - 1}{\beta}\right)\right) \tag{2b}$$

The QEI model, Eq. (2a) and (b), has the following inputs: $\Delta\theta$, ΔK, K_0, and S. All these inputs can be related to the soil hydraulic parameters (θ_r, θ_S, σ, h_{kg}, K_s) and the initial water content, θ_0. Sorptivity, S, can be computed from the soil hydraulic parameters using the formulation proposed by Parlange (1975):

$$S(\theta_0, \theta_r, \theta_s, \sigma, h_{kg}, K_s) = \sqrt{\int_{\theta_0}^{\theta_s} (\theta_s + \theta - 2\theta_0)\ D(\theta)\, d\theta} \tag{3a}$$

where the soil water diffusivity is given by

$$D(\theta) = K(\theta)\frac{dh}{d\theta} \tag{3b}$$

Given these equations, the quasi-exact implicit model can be written as a function of time, t, and the set of hydraulic parameters $I_{3D}(t) = I_{3D}(t, \theta_r, \theta_S, \sigma, h_{kg}, K_S)$. Considering that θ_r and θ_S are fixed, infiltration depends only on the hydraulic parameters h_{kg}, K_S, and σ. Consequently, the fit of the model to experimental data is performed to estimate h_{kg}, K_S, and σ using a specific inverting procedure, detailed below.

First, a random set of hydraulic parameters (σ, h_{kg}, K_S) are selected. Second, the inputs of the QEI model are computed from σ, h_{kg}, and K_S. The initial hydraulic conductivity, K_0, is computed from σ and K_S using the Kosugi hydraulic conductivity function defined in Table 1. The sorptivity, S (σ, h_{kg}, K_S), is computed using Eq. (3a). Then the observation data ($t_{obs,i}$, $I_{obs,i}$) are scaled on the basis of the following procedure (Lassabatere et al., 2009):

$$t^*_{obs,i} = \frac{2(\Delta K)^2}{S^2} t_{obs,i} \tag{4a}$$

$$I^*_{obs,i} = \frac{2\Delta K}{S^2}\left(I_{obs,i} - \left(K_0 + \frac{\gamma}{\check{r}\Delta\theta} S^2\right) t_{obs,i}\right) \tag{4b}$$

If the set of hydraulic parameters (σ, h_{kg}, K_S) were properly chosen, the obtained scaled data should verify Eq. (2). Consequently, a novel objective function, OF_{best_qei}, which assesses the difference between the right and left terms of Eq. (2b), is defined. It is important to note that the data set is split into two parts (the transient and the steady states), and the relative weights of these two states are determined by the value of w, in order to strengthen the inverting procedure to avoid the over-weights for the steady state:

$$\begin{aligned} OF_{\text{best\_qei}}(\sigma, h_{kg}, K_s) = {} & \frac{w}{N_{trans}} \sum_{i=1}^{i=N_{\text{trans}}} \left[(1-\beta) t^*_{obs,i} - \left(I^*_{obs,i} - \ln\left(\frac{\exp\left(\beta\, I^*_{obs,i}\right) + \beta - 1}{\beta}\right)\right)\right]^2 \\ & + \frac{(1-w)}{N_{stead}} \sum_{i=(N_{\text{trans}}+1)}^{i=N_{\text{end}}} \left[\log_{10}\left((1-\beta) t^*_{obs,i}\right) - \log_{10}\left(I^*_{obs,i} - \ln\left(\frac{\exp\left(\beta\, I^*_{obs,i}\right) + \beta - 1}{\beta}\right)\right)\right]^2 \end{aligned} \tag{5}$$

where i is the index of the infiltration data; N_{stead} and N_{trans} are the number of infiltration data for the transient and steady states, respectively; and N_{end} is the maximum number of data points.

Cumulative infiltration curves for observed and simulated are always closer (less discrepancy and smaller errors) at the beginning of the infiltration process, as for both curves $I(t=0) = 0$. In order to balance the fit along the entire infiltration process (transient and steady state), it is necessary to account for the fact that the accumulated errors between these infiltrations are larger for the steady state. Subsequently, if no transformation is performed for the steady state, then the fit would preferentially fit the steady state and overlook the transient state. Therefore, a $\log_{10}$ transformation is performed for the steady state, which allows the different order of magnitude between transient and steady-state errors to be compensated. For fine tuning, a weighting, w, is introduced with an optimal value of $w = 0.2$, obtained by trial and error.

The novelty of the proposed $OF_{\text{best\_qei}}$ is that it is not biased by the ratio of the number of observations in the steady and transient phases. The number of data points that belong to the transient and steady states is calculated by comparing the related time with the threshold $t_{\text{trans\_steady\_qei}}$ [T]. This threshold corresponds to the time at which the infiltration state passes from transient to steady. It is directly derived from the experimental cumulative infiltration curve, assuming that it separates the two parts of the curves that are concave and linear; these parts represent the transient and steady states, respectively. A linear regression is performed on the last points that align on the final straight

Table 2
Feasible range of the Kosugi and van Genuchten hydraulic parameters used for optimization. The value of θ_r is assumed to be 0 as in the original BEST method (Lassabatere et al., 2013). Values are based on Latorre et al. (2015) for K_S and on Pollacco et al. (2013a,b) for the Kosugi σ and h_{kg} as well as the van Genuchten n and h_{vg} parameters.

	Universal		Kosugi		van Genuchten	
	θ_r [cm^3 cm^{-3}]	$\log_{10} K_S$ [$\log_{10}$ (cm h^{-1})]	$\log_{10} h_{kg}$ [$\log_{10}$ (cm h^{-1})]	σ [–]	$\log_{10} h_{vg}$ [$\log_{10}$ (cm h^{-1})]	n [–]
Min	0	−2.14	1.2	0.8	0.30	1.09
Max	0	2.26	6.0	4.0	6.00	2.3

line, and the related slope and intercept are computed. Then, the next point (starting from the end) is interpolated and the following condition is tested:

$$\frac{I_{3D}(t) - I_{3D\_Interpolated}(t)}{\Delta T} \leq P_{transient\_steady} \quad (6)$$

where ΔT [T] is the time step for the cumulative infiltration data and $P_{transient\_steady}$ was fixed at a value of 0.05 mm s^{-1} obtained as a threshold representing the deviation from linearity. The procedure is stopped as soon as the equation is no longer valid, which highlights a too-strong deviation of the point from the straight line. The transition time is defined by the last point that validates Eq. (6).

The inverting procedure computes the objective function for several sets of hydraulic parameters. An optimization algorithm computes the optimum hydraulic parameters. Note that the objective function, OF_{best_qei}, involves three parameters and may suffer from non-uniqueness. A specific strategy is defined to reduce the number of parameters, and this is detailed in Section 2.3. Latorre et al. (2015) have already implemented the QEI model in their inversion algorithm. However, in this study the objective function is modified to improve the fitting procedure such that it is not biased by the ratio of the number of observations in the steady and transient phases.

2.2. A new, simplified, approximate expansion into the BEST method, $BEST_{SA}$

The $BEST_{QEI}$ algorithm implements the QEI model, but it needs to be solved numerically. Therefore a new simplified expansion based on the two-term approximation of Haverkamp et al. (1994) is proposed as follows:

$$I_{3D\_trans}(t) = S\sqrt{t} + \left(A\,S^2 + B\,K_s\right)t \quad (7a)$$

$$I_{3D\_steady}(t) = \left(A\,S^2 + K_s\right)t + C\frac{S^2}{K_s} \quad (7b)$$

The A [L^{-1}] parameter was already defined above, while constants B [–] and C [–] can be written as (Lassabatere et al., 2013):

$$A = \frac{\gamma}{\check{r}\Delta\theta} \quad (7c)$$

$$B = \frac{2-\beta}{3} + \frac{1+\beta}{3}\frac{K_0}{K_S} \quad (7d)$$

$$C = \frac{1}{2(1-\beta)\left(1-\frac{K_0}{K_S}\right)}\ln\left(\frac{1}{\beta}\right) \quad (7e)$$

In this new methodology the two approximate expansions, $I_{3D\_trans}(t)$ and $I_{3D\_steady}(t)$, are combined into a combined approximate function, $I_{3D\_SA}(t)$, referred to as the shifting approximation. This new expression automatically assigns the corresponding approximate function by comparing the time with the threshold shifting between the transient and steady states, $t_{trans\_stead\_SA}$. If time is higher than $t_{trans\_stead\_SA}$, the expression will compute the steady-state expansion; otherwise it will compute the transient-state expansion. The proposed shifting approximation model, $I_{3D\_SA}(t)$, can be written as follows:

$$I_{3D\_SA}(t) = \begin{cases} I_{3D\_trans}(t) = S\sqrt{t} + \left(A\,S^2 + B\,K_s\right)t & t \leq t_{trans\_steady\_SA} \\ I_{3D\_steady}(t) = \left(A\,S^2 + K_s\right)t + C & t > t_{trans\_steady\_SA} \\ t_{trans\_steady\_SA} = \left[\frac{S}{2(1-B)K_s}\right]^2 \end{cases} \quad (8)$$

This new version of BEST, referred to as $BEST_{SA}$, uses this new approximate expansion, which has the advantage of being defined for all times in contrast to the original BEST. The inverse modelling is performed in a similar way to that used for the $BEST_{QEI}$ method. The hydraulic parameters (σ, h_{kg}, K_S) are used to derive all the inputs needed for $I_{3D\_SA}(t)$, particularly the initial relative hydraulic conductivity, $\frac{K_0}{K_S}$, which is involved in constants B and C, as well as in the sorptivity, S (through Eq. (3a)). The modelled data are then compared to the experimental data using the objective function OF_{best_sa} (Eq. (9)). This objective function splits the data into transient and steady states, similar to OF_{best_qei}. The objective function is then minimized to define the optimum values of σ, h_{kg}, and K_S.

$$\begin{aligned} &OF_{best\_sa}(\sigma, h_{kg}, K_s) \\ &= w\frac{\sum_{t_i<t_{trans\_steady\_SA}}\left[I_{obs,i} - I_{3D\_SA}(t_i)\right]^2}{\sum_{t_i<t_{trans\_steady\_SA}}\left[I_{obs,i} - \overline{I_{obs,i}}\right]^2} \\ &+ (1-w)\frac{\sum_{t_i>t_{trans\_steady\_SA}}\left[\log_{10}\left[I_{obs,i}\right] - \log_{10}\left[I_{3D_SA}(t_i)\right]\right]^2}{\sum_{t_i>t_{trans\_steady\_SA}}\left[\log_{10}\left[I_{obs,i}\right] - \overline{\log_{10}\left[I_{obs,i}\right]}\right]^2} \end{aligned} \quad (9)$$

The relative weight, w, between the two terms of this objective function was found by trial and error to be equal to 0.5. The rationale for the logarithm transformation for the second term of the OF_{best_sa} is the same as for OF_{best_qei} (Eq. (5)), as described in Section 2.1.

2.3. Reducing the non-uniqueness of the Kosugi hydraulic parameters

The optimization of the hydraulic parameters using $BEST_{QEI}$ and $BEST_{SA}$ suffers from non-uniqueness when simultaneously inverting the three parameters (σ, h_{kg}, K_S). Therefore, it is proposed to reduce the non-uniqueness of the Kosugi parameters (σ, h_{kg}) considering the relationship between h_{kg} and σ found by Pollacco et al. (2013a).

According to Pollacco et al. (2013a), there is a positive linear correlation between h_{kg} and σ for most soils. Larger median pore size (small h_{kg}), which is characteristic of coarsely structured soils, is linked to a smaller standard distribution (dispersion) of the pore size (small σ). This relationship can be explained by the fact that when h_{kg} is small, the soil tends to be single-grain structured (monodisperse) and so σ tends to be small. On the other hand, when h_{kg} is increased, which is characteristic of finer material, the soil structure becomes aggregated or the soil is composed of an array of grain sizes (polydisperse), and so σ tends to have a larger dispersion. Pollacco et al. (2013a) obtained a root mean squared error of 0.45 using a dataset of 73 soils by using the following relationship between h_{kg} [cm] and σ [–]:

$$\sigma_{mod} = P_{\sigma 1}\left[\ln\left(h_{kg}/10\right) - 1\right]^{P_{\sigma 2}} \quad (10)$$

where $P_{\sigma 1} = 0.382$ and $P_{\sigma 2} = 1.080$ are fitting parameters.

Table 3
Target van Genuchten (VG) hydraulic parameters derived from Latorre et al. (2015) and the equivalent optimized Kosugi (KG) hydraulic parameters, related goodness of fits between $\theta(h)$ and $K(\theta)$, NSE_{θ_k}, and goodness of fits of analytical QEI and SA models fed with the optimized KG hydraulic parameters with respect to target cumulative infiltrations generated with HYDRUS (NSE_i). Shaded rows correspond to less accurate matches, in terms of both WRHCFs and cumulative infiltrations.

					VG		KG				QEI		SA	
ID	Soil type	θ_s [cm^3 cm^{-3}]	θ_r [cm^3 cm^{-3}]	K_S [cm h^{-1}]	h_{vg} [cm]	n [–]	h_{kg} [cm]	σ [–]	ΔK_{θ_s}	VG_KG NSE_{θ_k}	KG NSE_i	VG NSE_i	KG NSE_i	VG NSE_i
1	**Loam 1**	0.42	0.090	4.3	3.01 10^3	2.21	4.90 10^3	0.98	74.0	1.00	1.00	1.00	1.00	1.00
2	**Loam 2**	0.43	0.078	1.0	2.75 10^3	1.56	1.00 10^4	1.60	39.6	1.00	1.00	1.00	1.00	1.00
3	**Silty Clay Loam**	0.41	0.270	3.4	1.95 10^3	1.53	7.76 10^3	1.65	151.7	1.00	0.98	0.98	0.99	0.99
4	**Sandy Loam**	0.38	0.050	30.1	5.25 10^2	1.46	2.63 10^3	1.79	1520.9	0.99	0.96	0.96	1.00	0.99
5	**Silt**	0.46	0.034	0.3	6.31 10^3	1.37	4.79 10^4	2.00	20.1	0.99	1.00	1.00	1.00	1.00
6	**Silty Loam**	0.38	0.010	1.6	3.80 10^3	1.18	2.63 10^5	2.74	141.5	0.96	0.86	0.94	0.89	0.96
Average:											0.97	0.98	0.98	0.99

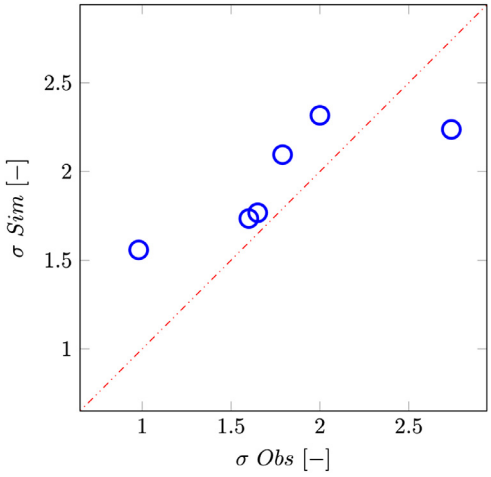

Fig. 1. Relationship between σ simulated and σ observed (Eq. (10)). Dotted line corresponds to the 1:1 line.

The optimization of the hydraulic parameters is therefore performed by optimizing only K_S and h_{kg} and deriving σ from σ_{mod} as shown in Fig. 1. The input parameters of Eqs. (4a), (b) and (8) that are used for the inversion procedure of BEST$_{QEI}$ and BEST$_{SA}$, respectively, are written as a function of ($\sigma_{mod}(h_{kg})$, h_{kg}, K_S) instead of (σ, h_{kg}, K_S). Thus, only h_{kg} and K_S are optimized.

3. Materials and methods

3.1. Synthetic soils and cumulative infiltrations

This study uses six contrasting synthetic soils investigated by Latorre et al. (2015) selected from the soil database of Carsel and Parrish (1988). Their WRHCFs are described using the van Genuchten (1980) model along with the Mualem condition ($k_m = 1$) and the Mualem (1976) capillary model. Related parameters are listed in Table 3 (VG column). The fit of these hydraulic functions with KG functions led to values of σ between 0.98 and 2.74.

Simulations from Latorre et al. (2015) were used to model water infiltration into these soils. These authors used a numerical domain 25 cm in radius and 25 cm in depth. The mesh is made of 100 (width) × 900 (height) elements. The vertical dimension of cells varies between 0.003 cm near the surface to 0.3 cm at the bottom. The cumulative infiltrations correspond to a disc radius of 10 cm. A null constant head was applied at the upper boundary below the ring, whereas a zero water-flux condition was applied to the rest of the boundary. Initial water content was fixed close to the residual water content. The maximum cumulative infiltration was fixed at 50 mm.

3.2. Equivalence between KG and VG WRHFCs and related hydraulic response

One of the crucial points of this work concerns the generality of the BEST methods. In this section we derive the KG WRHCFs from the VG WRHCFs. First, the target VG WRHCFs were fitted to the KG WRHCFs. The KG hydraulic parameters are derived from the VG parameters n and h_{vg} for the Mualem model ($k_m = 1$) by minimizing the objective function OF_{θ_kg}, which is based on the Nash-Sutcliffe efficiency formulation:

$$OF_{\theta\_kg} = w \frac{\sum_i^{i=N} \left[S_{e\_kg}(h_i) - S_{e\_vg}(h_i)\right]^2}{\sum_i^{i=N} \left[S_{e\_kg}(h_i) - \overline{S_{e\_kg}(h_i)}\right]^2} + (w-1)\frac{\sum_i^{i=N} \left[ln\, K_{r\_kg}(h_i) - \ln K_{r\_vg}(h_i)\right]^2}{\sum_i^{i=N} \left[ln\, K_{r\_kg}(h_i) - \overline{ln\, K_{r\_kg}(h_i)}\right]^2} \quad (11)$$

where w is a weighting parameter, which is equal to 0.5, as recommended by Pollacco et al. (2013a,b), and N is the number of discretised S_e data points, which is equal to 1000. The parameter w rules the relative weights assigned to the fits of the water retention curve and the hydraulic conductivity curve. The feasible range of parameters used for the fits is listed in Table 2. These values are based on Latorre et al. (2015) for K_S, and on Pollacco et al. (2013a,b) for the Kosugi σ and h_{kg}, as well as the van Genuchten n and h_{vg} parameters.

Second, the capability of the KG WRHCFs to predict the target cumulative infiltrations is evaluated. The optimized KG WRHCFs were used to compute the analytical QEI and SA models. These analytical data were compared to the numerically generated cumulative infiltration from Latorre et al. (2015). In addition to an adequate representation of the original $\theta(h)$ and $K(\theta)$, the optimized KG WRHCFs should provide similar cumulative infiltrations to those generated numerically using the VG WRHCFs. The agreement between analytically generated data using KG WRHCFs, $I_{sim}(t_i)$, and numerically generated data using the VG WRHCFs in the HYDRUS-3D model (Šimůnek et al., 2016), $I_{hydrus}(t_i)$, was assessed using the Nash-Sutcliffe efficiency coefficient, NSE_i, defined as follows:

$$NSE_i = 1 - \frac{\sum_{i=1}^{i=N} \left[I_{hydrus}(t_i) - I_{sim}(t_i)\right]^2}{\sum_{i=1}^{i=N} \left[I_{hydrus}(t_i) - \overline{I_{hydrus}(t_i)}\right]^2} \quad (12)$$

where N corresponds to the maximum number of infiltration data.

The computation of analytically generated data and the performance of the inverting procedure require the computation of S. The numerical

Table 4
Accuracy of fits (NSE_i), estimates for sorptivity (relative error as in Eq. (13), $Er(S)$), saturated hydraulic conductivity (relative error as in Eq. (13), $Er(K_S)$), and agreement between estimated and target WRHCFs (NSE_{θ_k}). Shaded rows correspond to less accurate matches.

		QEI (constrained with σ_{mod})				QEI (unconstrained)			BEST_SA (constrained with σ_{mod})			
ID	Soil type	NSE_i	$Er(S)$	$Er(K_S)$	NSE_{θ_k}	NSE_{θ_k}	$Er(S)$	$Er(K_S)$	NSE_i	$Er(S)$	$Er(K_S)$	NSE_{θ_k}
1	**Loam 1**	1.00	1.00	0.64	−1.81	−6.07	1.00	0.64	1.00	0.99	0.64	−1.84
2	**Loam 2**	1.00	0.99	0.73	0.66	0.58	0.99	0.73	1.00	0.98	0.74	0.66
3	**Silty Clay Loam**	1.00	0.86	0.94	0.93	−0.75	0.86	0.94	1.00	0.88	0.97	0.93
4	**Sandy Loam**	0.96	0.90	0.88	0.98	−5.16	0.90	0.88	1.00	0.96	0.88	0.97
5	**Silt**	1.00	0.99	0.34	0.92	0.63	0.99	0.34	1.00	0.98	0.24	0.84
6	**Silty Loam**	1.00	0.76	0.69	−0.05	−1.63	0.76	0.69	1.00	0.79	0.71	−0.02
Average		0.99	0.92	0.70	0.27	−2.07	0.92	0.70	1.00	0.93	0.70	0.26

integration of S (Eq. (3a) and (b)) is non-trivial because the integration is ill posed, since $\lim_{\theta\to\theta_s} D(\theta) \to +\infty$. Therefore, it is necessary to limit the highest soil water content to $\theta_{end} = \theta(S_e = 1 - 10^{-9})$. It was found that 10^{-9} is the smallest value before getting numerical instability. The integration was computed in Julia programming language using the QuadGK package (https://juliamath.github.io/QuadGK.jl/stable/).

3.3. Inverting procedure, related goodness of fit, and model accuracy

The global optimization of the hydraulic parameters was performed using a robust global optimizer BlackBoxOptim in Julia language (https://github.com/robertfeldt/BlackBoxOptim.jl). Due to the imposed constraints, it proved successful to use the local optimizer Optim.optimize (GoldenSection), also in Julia language (https://github.com/robertfeldt/BlackBoxOptim.jl) (Mogensen and Riseth, 2018), which is considerably faster than the global optimizer.

The goodness of fit of fitted modelled data, I_{sim}, to match the target numerically generated observations, I_{hydrus}, was assessed using the Nash-Sutcliffe efficiency formulation, NSE_i, described above. The accuracy of the different inverting procedures was evaluated considering the relative errors, Er, between estimated and target parameters:

$$Er(X) = 1 - \frac{\left|X_{est} - X_{target}\right|}{X_{target}} \tag{13}$$

where X_{est} and X_{target} are the values of any parameter estimated by the inverting procedure and the corresponding target, respectively. Note that the target values for the hydraulic parameters correspond to those derived from the previous fit of KG WRHCFs to the original VG WRHCFs.

4. Results and discussion

The validity of the new BEST method is assessed using the following steps: Section 4.1 demonstrates the capability of the optimized KG WRHCFs to fit the target VG WRHCFs. Section 4.2 shows that the QEI and the new BEST method parameterized with known VG and KG hydraulic parameters could reproduce the target cumulative infiltrations derived with the HYDRUS-3D model. Section 4.3.1 derives the accuracy of predicting *infiltration, transition time, saturated hydraulic conductivity* and *sorptivity* by inverting the hydraulic parameters of the QEI and the new BEST method with cumulative infiltration without constraining the hydraulic parameters (i.e., without using the relationship between σ and h_{kg}). Section 4.3.2 describes the accuracy of the QEI and the new BEST method to predict WRHCFs and the Kosugi hydraulic parameters by inverting the hydraulic parameters with cumulative infiltration by constraining the hydraulic parameters with the relationship between σ and h_{kg}.

4.1. Comparison between VG and KG WRHCFs

The capability of the optimized KG WRHCFs to fit observed VG WRHCFs is assessed and depicted in Fig. 2, with the related optimized parameters listed in Table 3 (columns "h_{kg}" and "σ"), along with the observed VG hydraulic parameters. The fits clearly align on the target curves in all cases (Fig. 2), and the related values of NSE_i attest to the quality of fits (Table 3, column "NSE_{θ_k}"). Although VG and KG correspond to different mathematical expressions, they can simulate similar hydraulic functions, in particular for $\sigma < 2$ or $n > 1.37$. The target curves are marginally less accurate for $\sigma > 2$, with a slight deviation at high suctions (Fig. 2, left). These results show that either VG or KG WRHCFs can be used to characterize the WRHCFs. For a more comprehensive comparison of VG and KG formulations, readers are referred to Assouline and Or (2013) and Cornelis et al. (2005).

4.2. Capability of known KG WRHCFs to reproduce target cumulative infiltrations computed with HYDRUS-3D

The capability of the optimized KG WRHCFs by using $BEST_{QEI}$ and $BEST_{SA}$ to reproduce the target cumulative infiltrations obtained with the HYDRUS-3D model (Šimůnek et al., 2016), $I_{hydrus}(t_i)$, is assessed. The KG parameters were used to compute the analytical model inputs (K_S, K_0, S) and the corresponding cumulative infiltration curves. Fig. 3 (left column) shows that both $BEST_{QEI\_KG}$ and $BEST_{SA\_KG}$ are very close to the target numerical cumulative infiltrations, $I_{hydrus}(t_i)$, for the case of *Loam 1, Loam 2*, and *Silt* ($\sigma = 0.98$, 1.60 and 2.00, respectively), with values of NSE_i coefficients equal to unity (Table 3, columns "QEI, KG, NSE_i" and "QEI, VG, NSE_i"). Conversely, the fits are less good, with lower values for the NSE_i coefficients but also close to unity for *Silty Loam* (σ = 2.74), *Silty Clay Loam* (σ = 1.65), and *Sandy Loam* (σ = 1.79).

Such inadequacy was already reported by Lassabatere et al. (2009), where discrepancies between analytical models and target numerical cumulative infiltrations were explained based on the failure of certain conditions needed for the QEI model (Haverkamp et al., 1994). In this study, an explanation for the discrepancy is based on the shape of the WRHCFs, and, in particular, the steep slope of $dK(S_e)/dS_e$ near saturation. To illustrate this, the indicator, ΔK_{θ_s}, is used:

$$\Delta K_{\theta_s} = \frac{K_s - K\left(S_e = 0.99\right)}{1 - S_e} \tag{14}$$

Table 3 shows that soils showing less good fit (*Silty Clay Loam* (σ = 1.65), *Sandy Loam* (σ = 1.79), and *Silty Loam* (σ = 2.74)) have large $\Delta K_{\theta_s} > 150\,cm\,h^{-1}$, and so the match between the analytical models and the real cumulative infiltration may be questionable for soils with $\Delta K_{\theta_s} > 150\,cm\,h^{-1}$, and further investigation may need to be conducted with experimental field data. However, the worst case in terms of agreement between WRHCFs and related cumulative infiltrations corresponds to *Silty Loam*, whereas the highest value for ΔK_{θ_s} is obtained for *Sandy Loam*. The proposed indicator for the mismatch between WRHCFs and related cumulative infiltrations may be combined in future research with alternative indicators. Lassabatere et al. (2009) proposed indicators

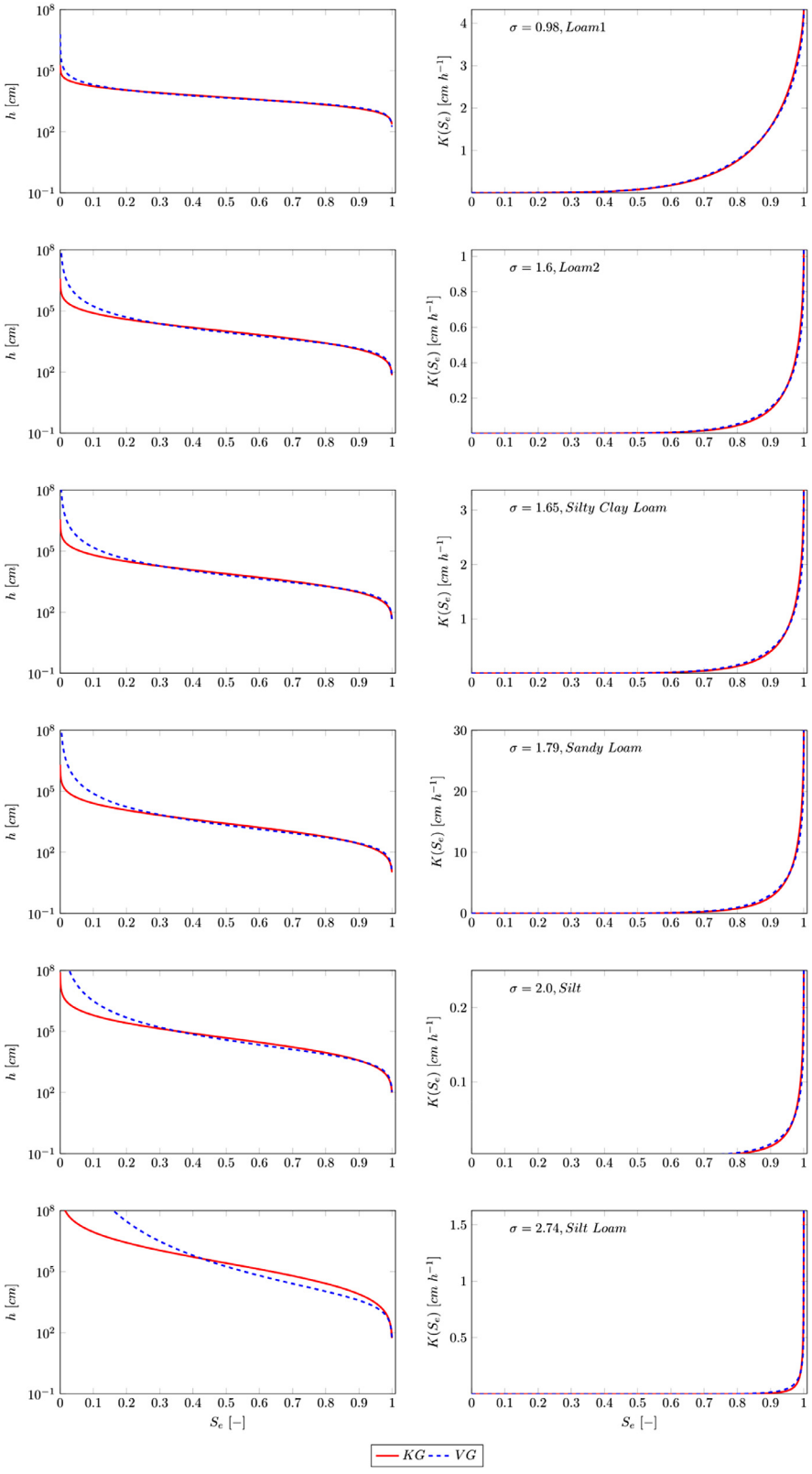

Fig. 2. $\theta(h)$ and $K(\theta)$ of VG and KG models showing a good match, especially for $\sigma < 2$. Soil type and corresponding σ values for the selected soils are indicated for each row in the right panel.

based on WRHCFs and the shape parameter, β, but this aspect will be the subject of further research.

For completeness, Fig. 3 (right column) shows good agreement between cumulative infiltration derived with BEST_{QEI} formulation using observed KG and VG hydraulic parameters. We conclude that the computed infiltration by using BEST_{QEI} and BEST_{SA} and hydraulic parameters for VG and KG matches accurately $I_{hydrus}(t_i)$ for soils with $\Delta K_{\theta_s} < 150\,\text{cm}\,\text{h}^{-1}$. Nevertheless, since BEST_{QEI} and BEST_{SA} have been tested with numerically generated data with HYDRUS-3D, the BEST_{QEI} and BEST_{SA} should be further tested with field experimental data.

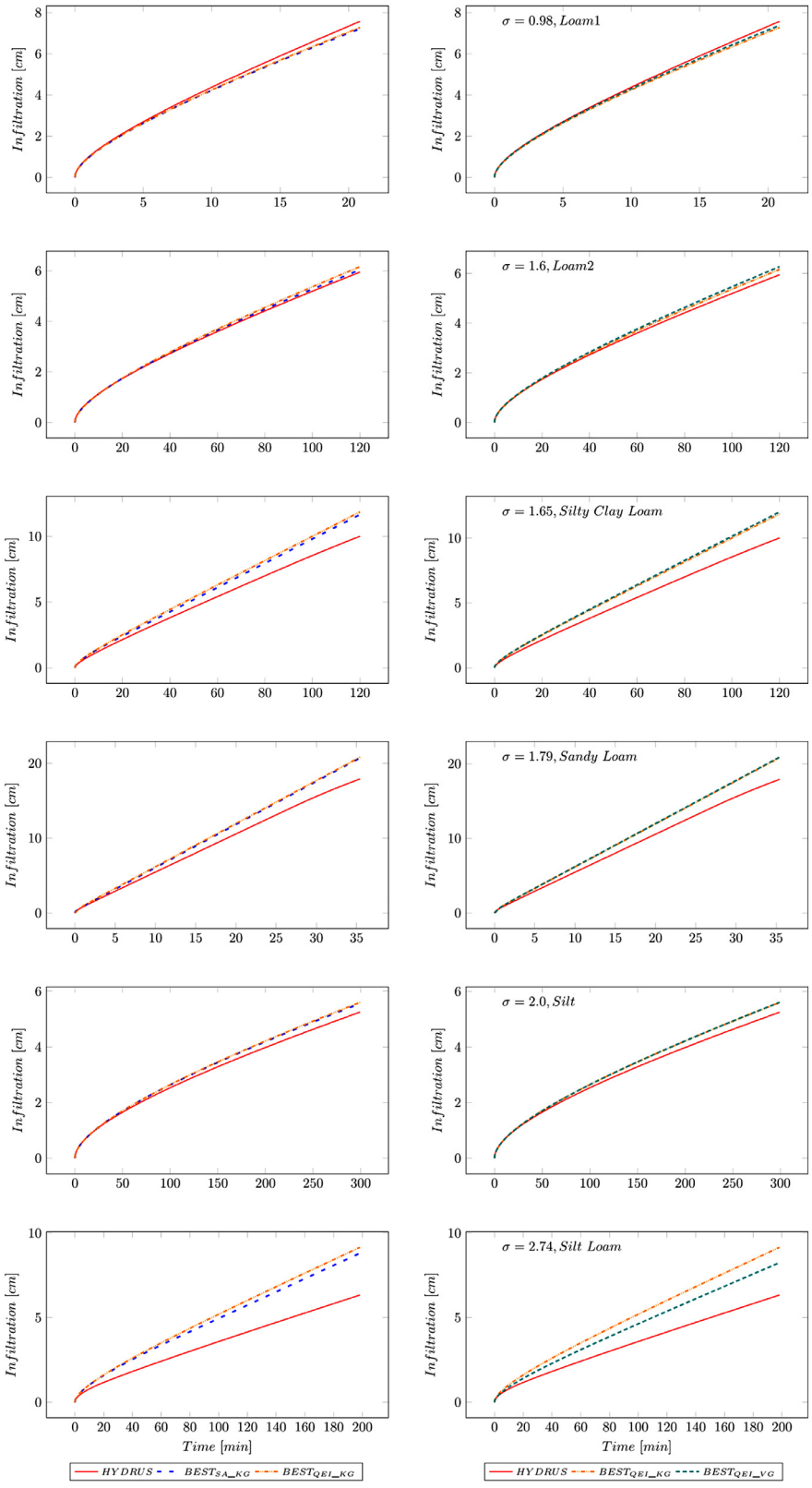

Fig. 3. Comparison between cumulative infiltration computed with the analytical QEI formulation (QEI) and the shifting approximation (SA) using the Kosugi (KG) hydraulic parameters (left column), and comparison between cumulative infiltration computed with the analytical QEI formulation (QEI) using the Kosugi (KG) and van Genuchten (VG) hydraulic parameters (right column). All panels include the target numerically generated cumulative infiltrations using HYDRUS. Soil type and corresponding σ values for the selected soils are indicated for each row in the right panel.

4.3. Accuracy of the inverted $BEST_{QEI}$ and $BEST_{SA}$

In the previous section the capability of KG WRHCFS to adequately model VG WRHCFs and the related computation of cumulative infiltration were investigated. This section uses the new $BEST_{QEI}$ and $BEST_{SA}$ methods to invert cumulative infiltrations and derive the corresponding WRHCFs and hydraulic parameters. The VG hydraulic parameters of the synthetic soils were used with the HYDRUS-3D software to numerically generate cumulative infiltrations, $I_{hydrus}(t_i)$, then infiltration data were inverted with $BEST_{QEI}$ and $BEST_{SA}$ to derive the

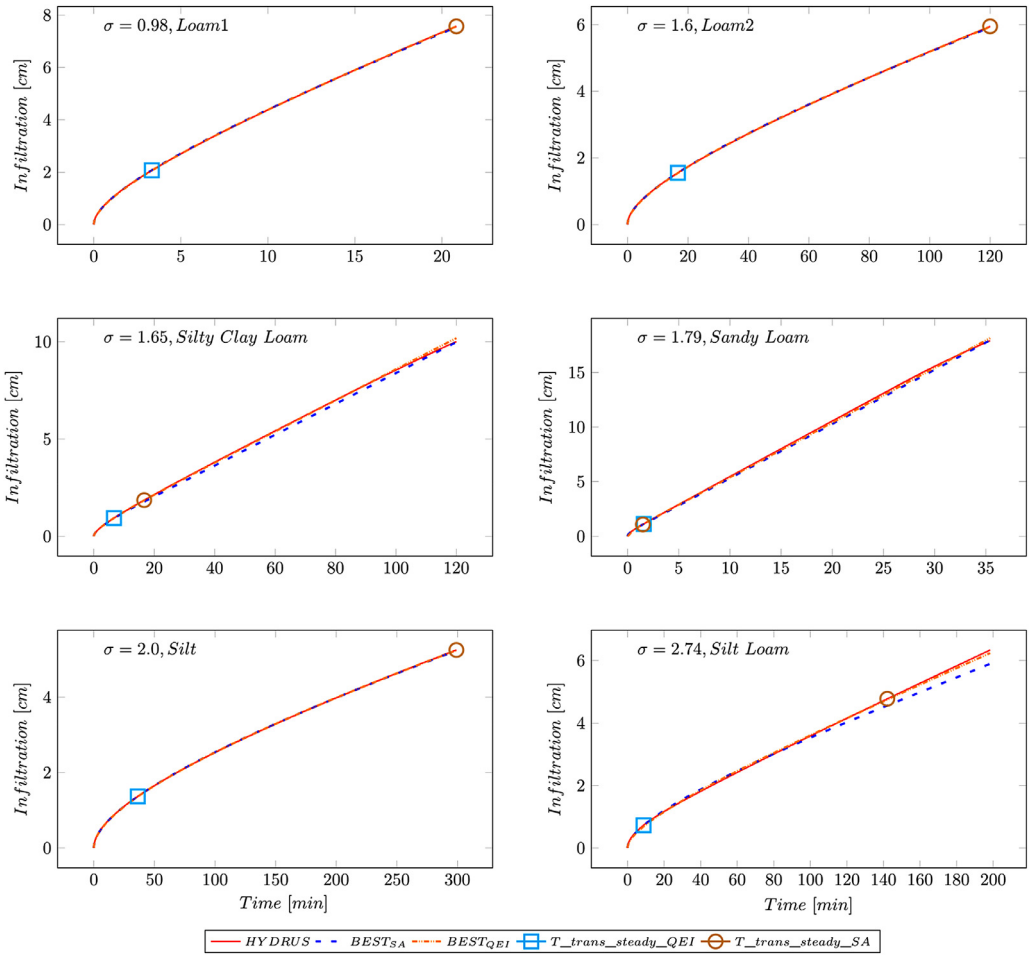

Fig. 4. Quality of fits of the target numerically generated data (HYDRUS) with $BEST_{QEI}$ and $BEST_{SA}$ methods. The threshold between the transient and steady states is depicted for the two methods ($t_{trans\_stead\_QEI}$ **and** $t_{trans\_stead\_SA}$).

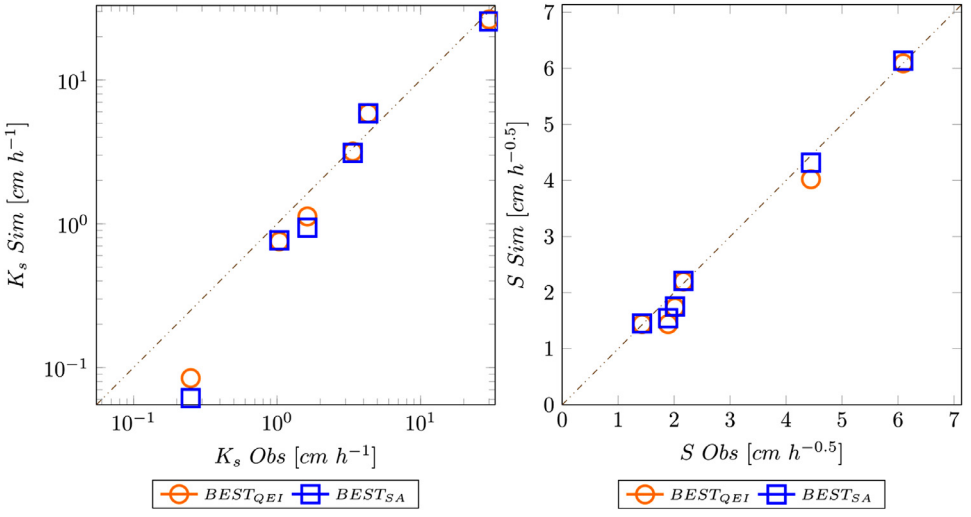

Fig. 5. Target and estimated saturated hydraulic conductivity (K_S) and sorptivity (S) with $BEST_{QEI}$ and $BEST_{SA}$ methods. Dotted lines correspond to the 1:1 line.

full set of hydraulic parameters and the related sorptivity. It is expected that both the estimated hydraulic parameters and the fits are less accurate for the cases of *Silty Clay Loam, Sandy Loam*, and *Silty Loam*, since the KG model has more difficulties depicting the target VG WRHCFs, and to model properly the corresponding cumulative infiltrations.

4.3.1. *Unconstrained optimization: without using relationship between σ and* h_{kg}

The use of the relationship between σ and h_{kg} (Eq. (10)) does not improve the predictions of infiltration, S and K_S since there is an infinite combination of σ and h_{kg} which gives similar values of S (Eq. (3a) and (b)) (their relative errors are equal for the constrained and uncon-

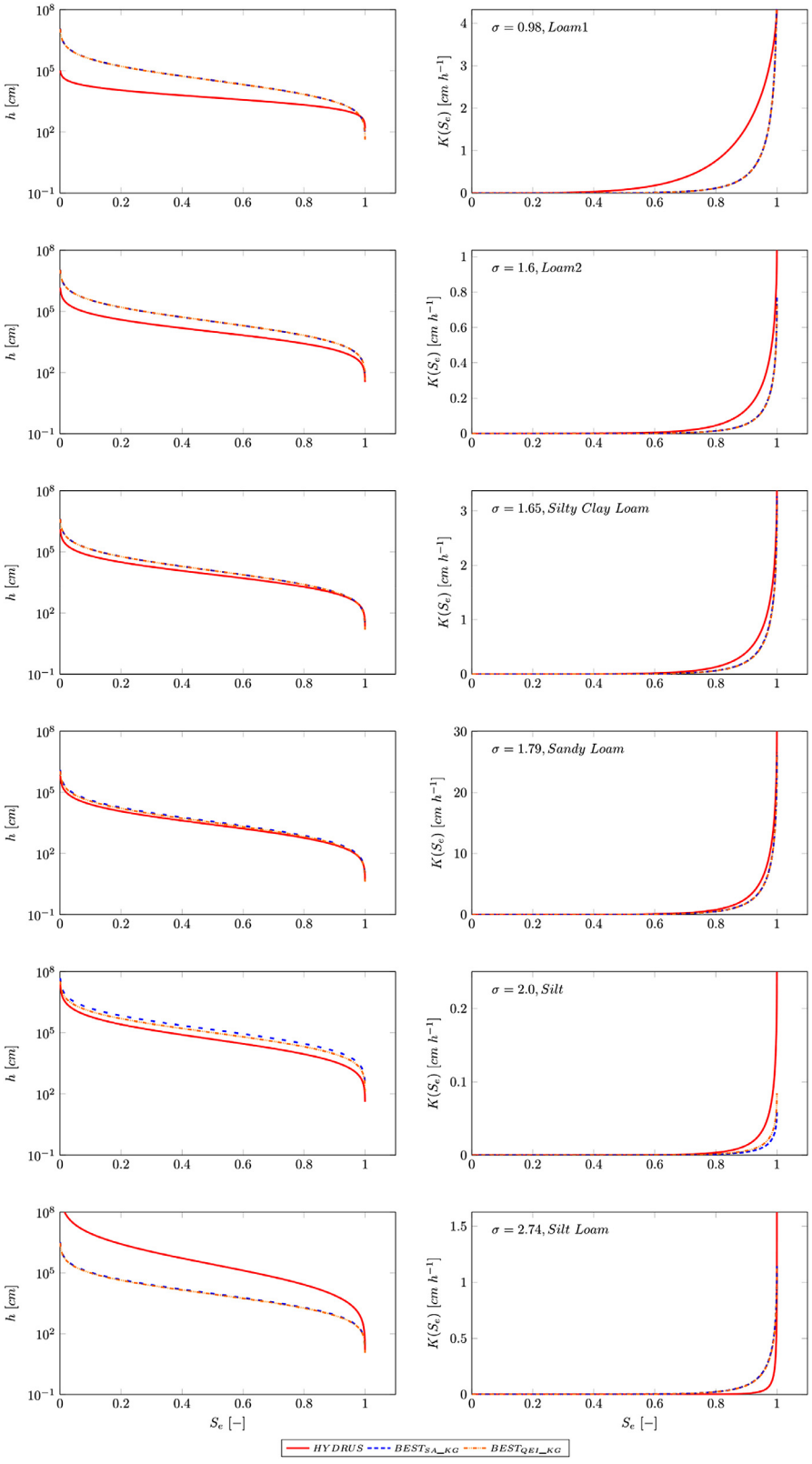

Fig. 6. Target (HYDRUS) and estimated WRHCFs by $BEST_{QEI}$ and $BEST_{SA}$ methods. Soil type and corresponding σ values for the selected soils are indicated for each row in the right panel.

strained case as shown in Table 4). However, this relationship is essential for a complete characterization of all the parameters.

4.3.1.1. Prediction of infiltration and transition time. Target cumulative infiltrations were properly modelled by the inverted hydraulic parameters obtained with $BEST_{QEI}$ and $BEST_{SA}$, as shown in Fig. 4. These results validate the methodology and prove the efficiency of both objectives functions, OF_{best_qei} and OF_{best_sa}.

However, the predicted transition times between the transient and steady states, t_{trans_stead}, are not always the same for $BEST_{QEI}$ and $BEST_{SA}$. The reason for this is that the BEST method assumes that infiltration in the steady state increases linearly with time (Eq. (7b)), while the QEI formulation does not because it considers the non-linear lateral flow.

Therefore, t_{trans_stead} of the BEST method is overestimated due to ignoring the non-linearity of the steady state. The inversion of infiltration data using $BEST_{QEI}$ and $BEST_{SA}$ is accurate, but t_{trans_stead} computed by $BEST_{QEI}$ is considered more realistic than computed by $BEST_{SA}$. In fact, $BEST_{SA}$ becomes linear faster than $BEST_{QEI}$ since $BEST_{SA}$ is an approximation of $BEST_{QEI}$ of order 2. This is why t_{trans_stead} is always smaller for $BEST_{QEI}$ than for $BEST_{SA}$.

4.3.1.2. Ability to predict K_S *and* s. K_S and S are depicted in Fig. 5. The results shown in Fig. 5 (left) and the values of $Er(K_S)$ listed in Table 4 confirm the predictions of K_S are accurate for both methods. Indeed, most of the points are close to the straight-line 1:1, indicating that estimated values are close to the targets. The estimates are comparable between $BEST_{QEI}$ and $BEST_{SA}$. The results shown in Fig. 5 (right) and $Er(S)$ (Table 4) confirm that the two methods $BEST_{QEI}$ and $BEST_{SA}$ perform well for the estimation of S, with estimates close to target values (similar results were obtained by Latorre et al., 2015). For most soils, $BEST_{SA}$ and $BEST_{QEI}$ have comparable estimates. Note that S is estimated with more accuracy than K_S (the scales are logarithmic for Fig. 5 (left) versus linear for Fig. 5 (right)). Lastly, the scattering of data points over both sides of the straight-line 1:1 on both subpanels of Fig. 5 demonstrates there is no trend to overestimate or underestimate the target. This is important, because it shows the methods do not systematically overestimate or underestimate parameters, meaning that they are not biased. With the data used, the predictions made with $BEST_{SA}$ are comparable to those made with $BEST_{QEI}$.

4.3.2. Constrained optimization: using relationship between σ *and* h_{kg}

4.3.2.1. Ability to predict WRHCFs. The quality of $BEST_{SA}$ and $BEST_{QEI}$ was assessed by comparing the estimated and target WRHCFs and analysing the values of the Nash-Sutcliffe efficiency coefficients, NSE_{θ_k}, (Table 4). Estimations of the WRHCFs are close to the target curves, in particular for *Loam 2, Silty Clay Loam, Sandy Loam*, and *Silt*. Larger discrepancies are found for *Loam 1* and *Silt Loam* (Figs. 5 and 6), with lower values of NSE_{θ_k} as shown in Table 4. For all considered soils, $BEST_{QEI}$ and $BEST_{SA}$ provide similar estimated WRHCFs. Less accurate estimates for some soils were expected, as stated above. It was proven that for some types of soils the computations of the cumulative infiltrations using the analytical models used by $BEST_{QEI}$ or $BEST_{SA}$ methods do not align on the target infiltration curves $I_{hydrus}(t_i)$. Consequently, the $BEST_{QEI}$ or $BEST_{SA}$ inverting procedure will compensate for such mismatch by mis-estimating the hydraulic parameters and related WRHCFs, deviating these far from the targets (Fig. 6).

Therefore, implementation of the relation between the scale parameter, h_{kg}, and the shape parameter, σ, strengthens the $BEST_{QEI}$ and $BEST_{SA}$ methods. The reduction in the number of optimizable parameters facilitates the inverting procedure. When three parameters are considered (σ, h_{kg}, K_S), the objective functions do not define a single minimum but a large zone. Then, depending on the initial values, the inverting algorithm may converge towards contrasting sets of optimized parameters, and probably contrasting WRHCFs. Conversely, the objective function related to $BEST_{QEI}$ and $BEST_{SA}$ is defined as a function of only two parameters (h_{kg}, K_S). The concomitant optimization of two parameters is less sensitive and more robust, leading to more accurate estimates. To demonstrate this, the data were inverted using the same framework for $BEST_{QEI}$ and $BEST_{SA}$ without any constraints (i.e. without the relation $\sigma_{mod}(h_{kg})$), resulting in worse results with lower values for the Nash-Sutcliffe efficiency coefficient NSE_{θ_k} (Table 4). In fact, the implementation of the relation between σ and h_{kg} through Eq. (10) in the $BEST_{QEI}$ and $BEST_{SA}$ methods is one of the main advantages of the methodologies.

The use of $\sigma_{mod}(h_{kg})$ enables predictions of WRHCFs for most soils in the absence of PSD. Improved predictions are foreseen when relationships of β are computed as a function of the WRHCFs, and when field experimental infiltration is used instead of that computed by HYDRUS-3D. This question has already been raised by Lassabatere et al. (2009), where the value of the β parameter, often fixed at 0.6, was questioned. Latorre et al. (2015) proved that the β parameter plays a role in modelling water infiltration data. Therefore, future studies will determine if varying β would improve the predictions of WRHCFs.

4.3.2.2. Ability to predict σ *and* h_{kg}. The accuracy of estimating σ and h_{kg} cannot be assessed because the estimated hydraulic parameters are related to KG functions, whereas target hydraulic parameters are related to VG functions. Consequently, the values of the hydraulic parameters cannot be directly compared. Moreover, the direct comparison of hydraulic parameters, even defined for similar functions, may be tricky. Pollacco et al. (2008) showed that there are equally good combinations of hydraulic parameters, which are “sets of truly linked parameters”. In other words, different combinations of σ and h_{kg} could produce a similar fit of $\theta(h)$ and $K(\theta)$ depicted in Fig. 6. It is expected that more physical σ and h_{kg} values would be obtained if they were further constrained from the relationship between K_S and hydraulic parameters related to $\theta(h)$ (Pollacco et al., 2013a, 2017). This issue will be the subject of further investigation. In the absence of PSD, the new BEST approach relying on Eq. (10) makes it possible to estimate these parameters, but we cannot be sure they correspond to the real values.

5. Conclusions

This paper develops two novel methods, $BEST_{QEI}$ and $BEST_{SA}$, which generalize the existing BEST methods to make predictions of any unimodal $\theta(h)$ and $K(\theta)$. In fact, these methods predict the WRHCFs on the basis of KG formulae, but it is demonstrated that these functions may depict any of the formulations for WRHCFs (including the VG type). KG functions were chosen because they are based on physical principles (log-normal distribution for pore size distributions). In the absence of PSD, the developed $BEST_{QEI}$ and $BEST_{SA}$ allow estimates of the full set of hydraulic parameters from the cumulative infiltration but require a link between the KG parameters (i.e., relationship between σ and h_{kg} as in Eq. (10)). This simplifies the procedures and avoids sources of errors due to the hypotheses behind the use of the pedotransfer functions of the previous BEST methods.

The developed new BEST methods are valid for all times and always manage to provide estimates, without any failure. This alleviates troubles and dysfunctions often encountered with the previous BEST methods. In addition, the objective functions of $BEST_{QEI}$ or $BEST_{SA}$ are improved, because they consider both transient and steady states and optimize their related contributions to the global objective function. Another novelty is the constraint implemented in these objective functions by defining the shape parameter, σ, as a function of the scale parameter for hydraulic pressure head, h_{kg}, as explained above.

The proposed $BEST_{QEI}$ and $BEST_{SA}$ methods were validated using numerically generated cumulative infiltrations with the HYDRUS-3D model for several synthetic soils. Following is a summary of the results.

Unconstraining the feasible parameter space:

- The predictions made with $BEST_{SA}$ are comparable to those made with $BEST_{QEI}$, but this needs further testing with real experimental data.
- Similar results were obtained by deriving the hydraulic parameters of KG and VG. These results suggest that $BEST_{QEI}$ and $BEST_{SA}$ methods are general, since they equally well represent any type of WRHCFs.
- The computed infiltration by using $BEST_{QEI}$ and $BEST_{SA}$ and observed hydraulic parameters accurately matches generated cumulative infiltration data with HYDRUS-3D for soils with a low gradient of hydraulic conductivity close to saturation. It is hypothesized that soils exhibiting specific hydraulic properties with high gradients could be inadequate for the use of the BEST model, as already discussed by Lassabatere et al. (2009). The $BEST_{QEI}$ and $BEST_{SA}$ should be further tested with real experimental data to settle this hypothesis.

- The inversion of infiltration by using $BEST_{QEI}$ and $BEST_{SA}$ is accurate, but t_{trans_stead} computed by $BEST_{QEI}$ is considered more realistic than that computed by $BEST_{SA}$.
- $BEST_{SA}$ and $BEST_{QEI}$ make accurate predictions of S and K_S, with S being predicted slightly more accurately than K_S.

Constraining the feasible parameter space:

- To constrain the feasible parameter space or make predictions without PSD, it is necessary to establish a relationship between the shape and scale hydraulic parameters (as in Eq. (10)).
- Although the predictions of WRHCFs are reasonable accurate for most soils, σ and h_{kg} exhibit "sets of truly linked parameters", and therefore their predictions are not unique. It is foreseen that more physical σ and h_{kg} values would be obtained with further constraints between K_S and the hydraulic parameters of the KG model.

6. Future work and recommendations to improve BEST

The new BEST procedure proves quite promising. However, additional research is needed to clarify the following points. The model has been tested with numerically generated data, and it should be further tested with real experimental data. In addition, experimental data could help to understand why some of the soils are less accurately characterized. It will be extremely useful to develop automated infiltrometers that allow both multiple replicate measurements and greater measurement precision during the transient state (particularly for soils with rapid infiltration), and that also allow cumulative infiltration to be sampled for large times (which is of interest for very low permeability soils). Automated infiltrometers often rely on use of pressure transducers with a Mariotte type water supply tank, however the bubbling within the Mariotte tank does introduce considerable uncertainty in the transducer readings, particularly under rapid infiltration during the transient phase. Water supply without the Mariotte design would greatly improve the precision of measurements. A key advantage of the BEST procedure is the simple equipment and measurement skills that allows estimation of a quantitative suite of WRHCF parameters, however this requires a high mathematical skill to derive these parameters from the field data. To achieve the potential widespread application of BEST measurements, easy to use software will need to be developed to allow uptake and application by non-soil physicists.

It will not be feasible to investigate the source of problems (e.g. inaccuracy of computing S) without performing an intensive field campaign, where infiltration tests are combined with measurements of hydraulic parameters in the laboratory and with 2D axisymmetric modelling of the flow below the infiltrometer (Réfloch et al., 2017). It is also recommended that infiltration experiments be combined with innovative non-invasive methods such as Ground Penetrating Radar, which can show the wetting front evolution with time during water infiltration (Iwasaki et al., 2016; Klenk et al., 2015; Leger et al., 2014a,b, 2015; Salas-García et al., 2017). Réfloch et al. (2017) also showed that monitoring the extension of the soil moisture stain around the infiltration ring with time is valuable for deriving the horizontal and vertical hydraulic parameters. The importance of compiling a worldwide data set with contrasting soils is clear, such as the SWIG database (Rahmati et al., 2018), particularly to improve the constraint of hydraulic parameters.

Lastly, analytical development is still needed to define more precisely the values of the infiltration parameters β and γ. Indeed, these were proved to depend on the type of soil (Lassabatere et al., 2009) and to have the potential to affect the values of estimates. Other approaches have aimed to relate these parameters to the WRHCFs (Fuentes et al., 1992). Improved predictions are also foreseen when the relationships of β and γ are obtained as a function of WRHCFs, or of the type of soils, and validated with experimental field data.

Conflicts of interest

There are no conflicts to declare.

Acknowledgements

This work was carried out as part of a scientific stay at Manaaki Whenua – Landcare Research in New Zealand, funded by a Salvador de Madariaga Mobility Grant awarded to J. Fernández-Gálvez by the Ministry of Education in Spain. The collaboration with ENTPE, France, was financed by Dumont d'Urville travel grants. Funding for Joseph Pollacco and Sam Carrick was provided by the New Zealand Ministry for Business, Innovation and Employment under the MBIE S-map Next Generation research programme. The authors also want to thank B. Latorre for sharing the HYDRUS-3D data and are grateful for the useful, detailed and constructive criticisms of the anonymous referees.

Supplementary material

Supplementary material associated with this article can be found, in the online version, at doi:10.1016/j.advwatres.2019.05.005.

References

Anderson, J.L., Bouma, J., 1973. Relationships between saturated hydraulic conductivity and morphometric data of an argillic horizon1. Soil Sci. Soc Am. J. 37, 408–413. https://doi.org/10.2136/sssaj1973.03615995003700030029x.

Angulo-Jaramillo, R., Bagarello, V., Lassabatere, L., 2016. Infiltration Measurements For Soil Hydraulic Characterization. Springer, Berlin Heidelberg, New York, NY.

Assouline, S., Or, D., 2013. Conceptual and parametric representation of soil hydraulic properties: a review. Vadose Zone J. 12, 0. https://doi.org/10.2136/vzj2013.07.0121.

Bagarello, V., Di Prima, S., Iovino, M., 2017. Estimating saturated soil hydraulic conductivity by the near steady-state phase of a Beerkan infiltration test. Geoderma 303, 70–77. https://doi.org/10.1016/j.geoderma.2017.04.030.

Bagarello, V., Di Prima, S., Iovino, M., 2014. Comparing alternative algorithms to analyze the Beerkan infiltration experiment. Soil Sci. Soc. Am. J. 78, 724. https://doi.org/10.2136/sssaj2013.06.0231.

Balland, V., Pollacco, J.A.P., 2008. Modeling soil hydraulic properties for a wide range of soil conditions. Ecol. Model. 219, 300–316.

Brooks, R.H., Corey, A.T., 1964. Hydraulic Properties of Porous Media. In: Hydraulic Properties of Porous Media. Colo. State Univ., Fort Collins, p. 27.

Carrick, S., Almond, P., Buchan, G., Smith, N., 2010. In situ characterization of hydraulic conductivities of individual soil profile layers during infiltration over long time periods. Eur. J. Soil Sci. 61, 1056–1069. https://doi.org/10.1111/j.1365-2389.2010.01271.x.

Carsel, R.F., Parrish, R.S., 1988. Developing joint probability distributions of soil water retention characteristics. Water Resour. Res. 24, 755–769.

Cornelis, W.M., Khlosi, M., Hartmann, R., Van Meirvenne, M., De Vos, B., 2005. Comparison of unimodal analytical expressions for the soil-water retention curve. Soil Sci. Soc. Am. J. 69, 1902. https://doi.org/10.2136/sssaj2004.0238.

Di Prima, S., 2015. Automated single ring infiltrometer with a low-cost microcontroller circuit. Comput. Electron. Agric. 118, 390–395. https://doi.org/10.1016/j.compag.2015.09.022.

Di Prima, S., Lassabatere, L., Bagarello, V., Iovino, M., Angulo-Jaramillo, R., 2016. Testing a new automated single ring infiltrometer for Beerkan infiltration experiments. Geoderma 262, 20–34. https://doi.org/10.1016/j.geoderma.2015.08.006.

Fuentes, C., Haverkamp, R., Parlange, J.-Y., 1992. Parameters constraints on closed-form soil water relationships. J. Hydrol. 134, 117–142. https://doi.org/10.1016/0022-1694(92)90032-Q.

van Genuchten, M.T., 1980. A closed-form equation for predicting the hydraulic conductivity of unsaturated soils. Soil Sci. Soc. Am. J. 44, 892–898.

Haverkamp, R., Parlange, J.-Y., Starr, J.L., Schmitz, G., Fuentes, C., 1990. Infiltration under ponded conditions: 3. A predictive equation based on physical parameters. Soil Sci. 149, 292.

Haverkamp, R., Ross, P.J., Smettem, K.R.J., Parlange, J.Y., 1994. Three-dimensional analysis of infiltration from the disc infiltrometer: 2. Physically based infiltration equation. Water Resour. Res. 30, 2931–2935. https://doi.org/10.1029/94WR01788.

Iwasaki, T., Kuroda, S., Saito, H., Tobe, Y., Suzuki, K., Fujimaki, H., Inoue, M., 2016. Monitoring infiltration process seamlessly using array ground penetrating radar. Agric. Environ. Lett. 1.

Klenk, P., Jaumann, S., Roth, K., 2015. Monitoring infiltration processes with high-resolution surface-based Ground-Penetrating Radar. Hydrol. Earth Syst. Sci. Discuss. 12, 12215–12246. https://doi.org/10.5194/hessd-12-12215-2015.

Kosugi, K., 1996. Lognormal distribution model for unsaturated soil hydraulic properties. Water Resour. Res. 32, 2697–2703. https://doi.org/10.1029/96wr01776.

van Looy, K., Bouma, J., Herbst, M., Koestel, J., Minasny, B., Mishra, U., Montzka, C., Nemes, A., Pachepsky, Y.A., Padarian, J., Schaap, M.G., Tóth, B., Verhoef, A., Vanderborght, J., van der Ploeg, M.J., Weihermüller, L., Zacharias, S., Zhang, Y., Vereecken, H., 2017. Pedotransfer functions in Earth system science: challenges and perspectives. Rev. Geophys. 55, 1199–1256. https://doi.org/10.1002/2017RG000581.

Lassabatere, L., Angulo-Jaramillo, R., Soria-Ugalde, J.M., Šimůnek, J., Haverkamp, R., 2009. Numerical evaluation of a set of analytical infiltration equations. Water Resour. Res. 45. https://doi.org/10.1029/2009WR007941.

Lassabatere, L., Angulo-Jaramillo, R., Ugalde, J.M.S., Cuenca, R., Braud, I., Haverkamp, R., 2006. Beerkan estimation of soil transfer parameters through infiltration experiments - BEST. Soil Sci. Soc. Am. J. 70, 521–532. https://doi.org/10.2136/sssaj2005.0026.

Lassabatere, L., Angulo-Jaramillo, R., Winiarski, T., Yilmaz, D., 2013. BEST method: characterization of soil unsaturated hydraulic properties. Adv. Unsaturated Soils 527–532.

Latorre, B., Peña, C., Lassabatere, L., Angulo-Jaramillo, R., Moret-Fernández, D., 2015. Estimate of soil hydraulic properties from disc infiltrometer three-dimensional infiltration curve. Numerical analysis and field application. J. Hydrol. 527, 1–12. https://doi.org/10.1016/j.jhydrol.2015.04.015.

Lauren, J.G., Wagnet, R.J., Bouma, J., Wosten, J.H.M., 1988. Variability of saturated hydraulic conductivity in a glossaquic hapludalf with macropores. Soil Sci. 145, 20.

Leger, E., Saintenoy, A., Coquet, Y., 2014a. Hydrodynamic parameters of a sandy soil determined by ground-penetrating radar inside a single ring infiltrometer. Water Resour. Res. 50, 5459–5474. https://doi.org/10.1002/2013WR014226.

Léger, E., Saintenoy, A., Coquet, Y., 2014b. Estimating saturated hydraulic conductivity from ground-based GPR monitoring Porchet infiltration in sandy soil. In: Ground Penetrating Radar (GPR), 2014 15th International Conference on. IEEE, pp. 124–130.

Léger, E., Saintenoy, A., Tucholka, P., Coquet, Y., 2015. Inverting surface GPR data to estimate wetting and drainage water retention curves in laboratory. In: Advanced Ground Penetrating Radar (IWAGPR), 2015 8th International Workshop on. IEEE, pp. 1–5.

McNeill, S.J., Lilburne, L., Carrick, S., Webb, T., Cuthill, T., 2018. Pedotransfer Functions for the Soil Water Characteristics of New Zealand Soils Using S-map Information. Geoderma Submitt..

Mogensen, P.K., Riseth, A.N., 2018. Optim: a mathematical optimization package for Julia. J. Open Source Softw. 3, 615. https://doi.org/10.21105/joss.00615.

Moret-Fernández, D., Latorre, B., 2017. Estimate of the soil water retention curve from the sorptivity and β parameter calculated from an upward infiltration experiment. J. Hydrol. 544, 352–362. https://doi.org/10.1016/j.jhydrol.2016.11.035.

Mualem, Y., 1976. A new model for predicting the hydraulic conductivity of unsaturated porous media. Water Resour. Res. 12, 513–522.

Nasta, P., Romano, N., Assouline, S., Vrugt, J.A., Hopmans, J.W., 2013a. Prediction of spatially variable unsaturated hydraulic conductivity using scaled particle-size distribution functions: simultaneous Scaling. Water Resour. Res. 49, 4219–4229. https://doi.org/10.1002/wrcr.20255.

Nasta, P., Romano, N., Chirico, G.B., 2013b. Functional evaluation of a simplified scaling method for assessing the spatial variability of soil hydraulic properties at the hillslope scale. Hydrol. Sci. J. 58, 1059–1071. https://doi.org/10.1080/02626667.2013.799772.

Parlange, J., 1975. Determination of soil-water diffusivity by sorptivity measurements. Soil Sci. Soc. Am. J. 39, 1011–1012. https://doi.org/10.2136/sssaj1975.03615995003900050057x.

Parlange, J.-Y., Lisle, I., Braddock, R.D., Smith, R.E., 1982. The three-parameter infiltration equation. Soil Sci. 133, 337–341.

Patil, N.G., Singh, S.K., 2016. Pedotransfer functions for estimating soil hydraulic properties: a review. Pedosphere 26, 417–430. https://doi.org/10.1016/S1002-0160(15)60054-6.

Pollacco, J.A.P., 2008. A generally applicable pedotransfer function that estimates field capacity and permanent wilting point from soil texture and bulk density. Can. J. Soil Sci. 88, 761–774.

Pollacco, J.A.P., Nasta, P., Ugalde, J.M.S., Angulo-Jaramillo, R., Lassabatere, L., Mohanty, B.P., Romano, N., 2013a. Reduction of feasible parameter space of the inverted soil hydraulic parameters sets for Kosugi model. Soil Sci. SS-S-12-00268.

Pollacco, J.A.P., Mohanty, B.P., Efstratiadis, A., 2013b. Weighted objective function selector algorithm for parameter estimation of SVAT models with remote sensing data. Water Resour. Res. 49, 6959–6978. https://doi.org/10.1002/wrcr.20554.

Pollacco, J.A.P., Ugalde, J.M.S., Angulo-Jaramillo, R., Braud, I., Saugier, B., 2008. A Linking Test to reduce the number of hydraulic parameters necessary to simulate groundwater recharge in unsaturated soils. Adv. Water Resour. 31, 355–369. https://doi.org/10.1016/j.advwatres.2007.09.002.

Pollacco, J.A.P., Webb, T., McNeill, S., Hu, W., Carrick, S., Hewitt, A., Lilburne, L., 2017. Saturated hydraulic conductivity model computed from bimodal water retention curves for a range of New Zealand soils. Hydrol. Earth Syst. Sci. 21, 2725–2737. https://doi.org/10.5194/hess-21-2725-2017.

Rahmati, M., Weihermüller, L., Vanderborght, J., Pachepsky, Y.A., Mao, L., Sadeghi, S.H., Moosavi, N., Kheirfam, H., Montzka, C., Looy, K.V., Toth, B., Hazbavi, Z., Yamani, W.A., Albalasmeh, A.A., Alghzawi, M.Z., Angulo-Jaramillo, R., Antonino, A.C.D., Arampatzis, G., Armindo, R.A., Asadi, H., Bamutaze, Y., Batlle-Aguilar, J., Béchet, B., Becker, F., Blöschl, G., Bohne, K., Braud, I., Castellano, C., Cerdà, A., Chalhoub, M., Cichota, R., Císlerová, M., Clothier, B., Coquet, Y., Cornelis, W., Corradini, C., Coutinho, A.P., Oliveira, M.B.de, Macedo, J.R.de, Durães, M.F., Emami, H., Eskandari, I., Farajnia, A., Flammini, A., Fodor, N., Gharaibeh, M., Ghavimipanah, M.H., Ghezzehei, T.A., Giertz, S., Hatzigiannakis, E.G., Horn, R., Jiménez, J.J., Jacques, D., Keesstra, S.D., Kelishadi, H., Kiani-Harchegani, M., Kouselou, M., Kumar Jha, M., Lassabatere, L., Li, X., Liebig, M.A., Lichner, L., López, M.V., Machiwal, D., Mallants, D., Mallmann, M.S., Marques, O., De, J.D., Marshall, M.R., Mertens, J., Meunier, F., Mohammadi, M.H., Mohanty, B.P., Pulido-Moncada, M., Montenegro, S., Morbidelli, R., Moret-Fernández, D., Moosavi, A.A., Mosaddeghi, M.R., Mousavi, S.B., Mozaffari, H., Nabiollahi, K., Neyshabouri, M.R., Ottoni, M.V., Filho, O., Benedicto, T., Pahlavan-Rad, M.R., Panagopoulos, A., Peth, S., Peyneau, P.-E., Picciafuoco, T., Poesen, J., Pulido, M., Reinert, D.J., Reinsch, S., Rezaei, M., Roberts, F.P., Robinson, D., Rodrigo-Comino, J., Filho, R., Corrêa, O., Saito, T., Suganuma, H., Saltalippi, C., Sándor, R., Schütt, B., Seeger, M., Sepehrnia, N., Sharifi Moghaddam, E., Shukla, M., Shutaro, S., Sorando, R., Stanley, A.A., Strauss, P., Su, Z., Taghizadeh-Mehrjardi, R., Taguas, E., Teixeira, W.G., Vaezi, A.R., Vafakhah, M., Vogel, T., Vogeler, I., Votrubova, J., Werner, S., Winarski, T., Yilmaz, D., Young, M.H., Zacharias, S., Zeng, Y., Zhao, Y., Zhao, H., Vereecken, H., 2018. Development and analysis of the Soil Water Infiltration Global database. Earth Syst. Sci. Data 10, 1237–1263. https://doi.org/10.5194/essd-10-1237-2018.

Réfloch, A., Gaudet, J.-P., Oxarango, L., Rossier, Y., 2017. Estimation of saturated hydraulic conductivity from ring infiltrometer test taking into account the surface moisture stain extension. J. Hydrol. Hydromech. 65. https://doi.org/10.1515/johh-2017-0019.

Salas-García, J., Garfias, J., Martel, R., Bibiano-Cruz, L., 2017. A low-cost automated test column to estimate soil hydraulic characteristics in unsaturated porous media. Geofluids 2017.

Šimůnek, J., Genuchten, M.T.van, Šejna, M., 2016. Recent developments and applications of the HYDRUS computer software packages. Vadose Zone J. 15. https://doi.org/10.2136/vzj2016.04.0033.

Smettem, K.R.J., Parlange, J.Y., Ross, P.J., Haverkamp, R., 1994. Three-dimensional analysis of infiltration from the disc infiltrometer: 1. A capillary-based theory. Water Resour. Res. 30, 2925–2929. https://doi.org/10.1029/94WR01787.

Varado, N., Braud, I., Ross, P.J., Haverkamp, R., 2006. Assessment of an efficient numerical solution of the 1D Richards' equation on bare soil. J. Hydrol. 14.

Yilmaz, D., Lassabatere, L., Deneele, D., Angulo-Jaramillo, R., Legret, M., 2013. Influence of carbonation on the microstructure and hydraulic properties of a basic oxygen furnace slag. Vadose Zone J. 12. https://doi.org/10.2136/vzj2012.0121.